Urban Air Mobility Communication Performance Considering Cochannel Interference

NOUR EL-DIN SAFWAT
ROBERTO SABATINI
ALESSANDRO GARDI
Khalifa University of Science and Technology, Abu Dhabi, UAE

ISMAIL MOHAMED HAFEZ
October 6 University, Giza, Egypt

FATMA NEWAGY
Ain Shams University, Cairo, Egypt

Urban air mobility (UAM) aims to establish a low-altitude transportation system that operates safely and efficiently to mitigate the increasing ground traffic congestion in densely populated areas. Various aircraft types, including passenger aerial vehicles and unmanned aerial vehicles, will be used to provide UAM services. In this context, a large number of aircraft are expected to operate in close proximity to each other, leading to challenges in terms of communication throughput and interference. To address these challenges, this article examines UAM communication requirements and the potential applications of cellular networks in the relevant flight environments. UAM wireless connectivity performance is analyzed focusing on cochannel interference and the mathematical expressions for the probability of coverage (PoC) are derived using stochastic geometry. Based on these premises, the improvements in PoC attainable using interference mitigation techniques, such as frequency reuse (FR) and separation distance (SD), are investigated. Then, a PoC enhancement algorithm is presented using a combined FR-SD method. Numerical verification case studies are performed in representative conditions, showing that the proposed method is able to mitigate cochannel interference, significantly reducing computational time and increasing spectrum efficiency.

Manuscript received 27 November 2023; revised 5 February 2024; accepted 1 April 2024. Date of publication 8 April 2024; date of current version 9 August 2024.

DOI. No. 10.1109/TAES.2024.3386150

Refereeing of this contribution was handled by J. Choi.

This work was supported by KU FSU-2022-013 Grant.

Authors' addresses: Nour El-Din Safwat, Roberto Sabatini, and Alessandro Gardi are with the Department of Aerospace Engineering, Khalifa University of Science and Technology, Abu Dhabi 127788, UAE, E-mail: (noureldin.mansour@ku.ac.ae; roberto.sabatini@ku.ac.ae; alessandro.gardi@ku.ac.ae); Ismail Mohamed Hafez is with the College of Engineering, October 6 University, Giza 12585, Egypt, E-mail: (imhafez.eng@o6u.edu.eg); Fatma Newagy is with the Department of Electronics and Communication, Faculty of Engineering, Ain Shams University, Cairo 11566, Egypt, E-mail: (fatma_newagy@eng.asu.edu.eg). *(Corresponding author: Roberto Sabatini.)*

I. INTRODUCTION

The remarkable expansion of the unmanned aerial vehicle (UAV) industry has given rise to a multitude of applications across diverse sectors [1], [2], [3]. In the realm of surveillance, UAVs serve as pivotal instruments, facilitating extensive terrain monitoring and enhancing security protocols. Agricultural practices benefit significantly from UAV precision, encompassing precision farming, ongoing crop monitoring, and systematic assessment of crop health. Search and rescue operations strategically leverage the nimble mobility of UAVs, proving instrumental in swift coverage of challenging terrains. The crucial role of UAVs extends to disaster management, contributing real-time imagery for nuanced damage assessments.

Furthermore, UAVs play a strategic role in communication networks, particularly in remote and emergency scenarios, thereby reinforcing connectivity. In logistics, UAV deployment ensures the prompt and streamlined delivery of medical supplies and goods. Notably, the application of UAVs in urban air mobility (UAM) represents a transformative paradigm, fundamentally reshaping transportation dynamics in urban area.

UAM is one of the advanced air mobility concepts that provide a safe and efficient air transportation system for goods and people in urban populated areas. The UAM concept of operations envisions a future where aerial vehicles play a pivotal role in alleviating traffic congestion and providing efficient transportation solutions within densely populated cities [4], [5], [6].

Developing a sustainable UAM sector requires an integrated approach based on the three main pillars: aircraft and aerial systems, infrastructure, and airspace and traffic management [7]. Concerning aircraft and aerial systems, the widespread adoption of electric vertical takeoff and landing (eVTOL) will be a distinctive characteristic of the UAM industry compared with the conventional aviation. In particular, innovative eVTOL configurations will provide new opportunities for passenger transport in cities, so different designs of eVTOL have been proposed, including tilt thrust, tail sitters, cruise lift, and cruise multirotor. Thus, NASA provides reference vehicles that aim to represent the variety of vehicle configurations presented across the UAM community [8], [9], [10], [11]. Each design has different characteristics and benefits depending on the targeted mission profile.

The infrastructure of UAM entails aerodromes and vertiports, which are strategically located within metropolitan areas, guided by factors, such as anticipated demand, zoning ordinances, environmental constraints, and stakeholder input. These ground facilities come in various types, including

those with runways and those requiring VTOL, serving different needs within urban centers. These aerodromes provide essential utilities, adhere to regulatory codes, and integrate with other transportation modes. Surveillance, navigation, and communication infrastructure are tailored to their unique environments, with provisions for emergency landings and redundancy. UAM aerodromes play a pivotal role in supporting passenger and cargo traffic by UAM vehicles (UVs), offering fast-charging and fuel options, while their physical and cybersecurity are managed by operators in compliance with relevant regulations.

Ensuring suitable airspace and traffic management services is essential for UAMs safe and efficient operation [12]. Consequently, NASA provided a scheme for UAM maturity levels (UML) [3] that classifies the UAM evolution into six levels. Each UML is defined by operational density, complexity, and the extent of reliance on automation. UAM is supposed to operate at UML-4 [3]. This level of maturity is projected to make UAM feasible in numerous metropolitan areas, and this feasibility is facilitated by the implementation of advanced communications, navigation, and surveillance and avionics (CNS+A) technologies and services.

The urban environment imposes limitations on low-altitude CNS systems, including challenges related to the obstruction of communication and global navigation satellite system signals caused by urban infrastructure [13], [14]. Additionally, very high frequency (VHF) voice communications and automatic dependent surveillance broadcast (ADS-B) are currently at maximum capacity in high-traffic airports. They would be insufficient to accommodate the anticipated increase in air traffic [15], [16]. Therefore, UAM requires new communication technologies to support high-density operations in urban environments.

A. Related Work

Within the realm of UAM, a large number of aircraft are expected to operate in proximity, posing challenges in communication connectivity between UV and cellular base station (CBS) and interference. In [17], the connectivity analysis for UAM between UV and CBS was presented; however, this analysis focuses on predicting turbulence using a neural network. The interference management techniques for UAVs were proposed in [18], [19], [20], [21], [22], and [23]. The cooperative interference cancelation (CIC) strategies were proposed in [18] and [19]. A decode and forward (DF) method for multibeam UAV to avoid cochannel interference was proposed in [18]. In [19], a quantize and forward (QF) based CIC method for uplink communication was presented. Lu et al. [20] proposed a scheme using the cloud radio access networks, spatial multiplexing, and beamforming to mitigate interference. In [21], the cooperative non-orthogonal multiple access (NOMA) was proposed to avoid uplink interference. The NOMA algorithm to reduce cochannel interference for cellular-connected UAV was presented in [22]. However, these techniques require high processing power, which increases the power consumption of the UAVs battery. Oubbati et al. [23] proposed a framework for minimizing energy consumption and maximizing throughput using deep reinforcement learning. However, the system's complexity poses a challenge. Therefore, we suggest a combined method utilizing both frequency reuse (FR) and separation distance (SD) to enhance probability of coverage (PoC) while simultaneously reducing cochannel interference. This integrated FR-SD method also demands lower complexity and processing power compared with the previously mentioned methods. Nevertheless, the proposed method faces limitations based on the available number of frequencies for reuse. Table I provides a comparison between our proposed method and the aforementioned approaches.

B. Contributions and Structure

This article presents a study of UAM communication requirements, considering cellular networks as a key technology enabler in addressing communication performance and challenges. Then, an analysis of UAM wireless connectivity performance is conducted focusing on cochannel interference between UVs and CBS. Using stochastic geometry, mathematical expressions for the PoC are derived and the improvement in PoC attainable using interference mitigation techniques, such as FRs and SD, is investigated. Then, an enhanced PoC algorithm is presented using combined FR-SD method.

The rest of this article is organized as follows. Section II presents UAM communication requirements. The system model is presented in Section III. The proposed PoC enhancement algorithm is presented in Section IV. Section V presents the numerical simulation results and associated discussion. Finally, Section VI concludes this article.

II. COMMUNICATION REQUIREMENTS

In urban environments, communication systems face significant challenges. VHF voice communications and ADS-B are already reaching their capacity limits, and these systems would struggle to accommodate the influx of new vehicles. The presence of urban structures, such as buildings, bridges, and towers, acts as substantial barriers to signal reception, ultimately compromising the reliability of communication. Additionally, urban areas are characterized by numerous reflective surfaces, which give rise to an increased prevalence of multipath signals, resulting in errors in received signals. Thus, UAM requires communication technologies that can support high-density operations in densely inhabited urban environments. Various UAM applications have different data rate prerequisites. Voice and basic command and control communications are able to operate at lower data rates. However, remote pilot operation and autonomous technology require higher data rates (up to 100 Mbps) [24]. A reliability requirement of 99.999% is necessary for navigation and surveillance [25]. In addition to that, due to the fast pace of operations and shorter characteristic distances compared with the conventional aviation, UAM requires low-latency communication, as low as 10 ms

TABLE I
Comparison of the Related Approaches and the FR-SD Method

Method	Technique	Main Advantage	Main Limitation
DF [18]	Multi-beam UAV CIC	Mitigating cochannel interference	Computational load
QF [19]			
Spatial multiplexing and beamforming [20]	Uses cloud radio access networks, spatial multiplexing, and beamforming		
NOMA [21], [22]	Based on NOMA		
TEAM framework [23]	Intelligent trajectories of multi-UAVs using deep reinforcement learning	Minimize energy consumption and maximize throughput	Complexity of the system
FR-SD method	FR and separation distance	Mitigating cochannel interference and maximizing coverage with low computational load	Limited by the available number of frequencies

[26]. Moreover, the dynamic nature of UAM and the abundance of obstacles in urban areas necessitate technologies capable of achieving communication beyond line-of-sight and effectively addressing specific line-of-sight issues in urban environments.

A. Cellular Communications for UAM

Cellular communications are promising state-of-the-art and rapidly evolving technologies that are adequate to fulfill UAM requirements of low-latency and high-throughput wireless connectivity [27]. For instance, 5G cellular communications boast a peak data throughput of 10 gigabits/s, which is ten times higher than 4G ones. When comparing potential network speeds between 5G and 6G technology, it is anticipated that 6G will be faster than 5G by 100 times, with improved dependability and network coverage [28]. Furthermore, both 5G and 6G utilize midband and high-band frequency spectrums for high-speed data transmission. The sub-6 GHz and over 24.25 GHz [29] are reserved for 5G and 6G, respectively. Additionally, 6G is expected to operate in the frequency band from 95 GHz to 3 THz, enabling the cellular network to provide "connectivity for the sky" through integration with satellites and aerial vehicles.

In normal conditions, 5G network latency is 10 ms, which is ten times lower than 4G. With 6G, latency is projected to drop to 1 ms, ten times lower than that of a 5G network, making it more suitable for UAMs low-latency communication requirements [30]. In terms of mobility, 5G networks provide satisfactory service at speeds of up to 500 km/h, compared with 350 km/h for 4G. In 6G, it is expected to support speeds of up to 1000 km/h [31]. Ultradense heterogeneous networks are supported in 6G with connection densities up to 10^7 devices/km^2 higher ten times than 5G [32]. The network performance comparison among 4G, 5G, and 6G is summarized in Fig. 1. The 6G exhibits promising network performance; however, it is still under research. Thus, 5G demonstrates acceptable performance, which can be a key enabler for UAM communications.

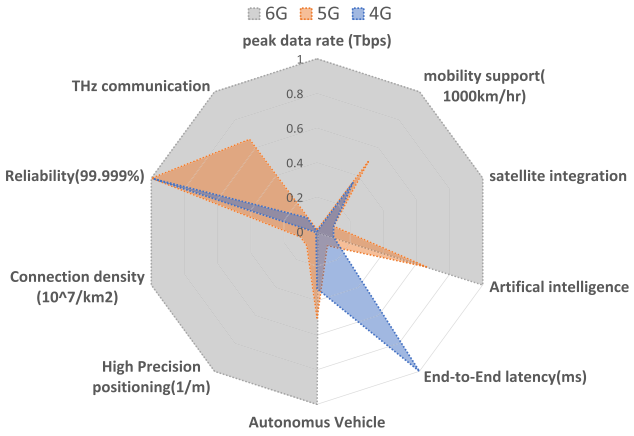

Fig. 1. 4G, 5G, and 6G network performance aspects.

B. Cellular Communication Challenges

1) *Network Infrastructure:* One challenge that limits the application of existing cellular networks to aerial vehicles is the downward-oriented antenna coverage pattern, as the cellular network is designed to cover ground users. Consequently, addressing this limitation requires either reconfiguring the existing CBS or establishing a dedicated CBS tailored to the needs of UAM communications, especially for UVs. The current CBS can be reconfigured by adding up-tilting antennas to serve UVs while considering the effect of antenna back lobes on the service provided to ground users [33]. Moreover, constructing a dedicated 5G network to offer stable 5G connectivity for UAM can significantly benefit from using 3-D network coverage optimization [34] and network slicing technology [35].

Tethered UAV (TUAV) and high-altitude platforms (HAPs) can be utilized as relays to connect cellular networks with UVs and to provide wide area coverage [36], [37]. TUAV is a low-altitude platform (LAP) supplied with power and data by a cable from a ground station to achieve the endurance and backhaul link quality requirements. However, the mobility and flexibility of TUAVs are restricted by their cable length. HAPs, on the other hand, offer greater flexibility and wider coverage due to operating above conventional

air traffic, making them an appealing solution with reliable communication technologies for UVs. Nonetheless, due to their greater distance from the user terminals, the use of HAPs would likely result in increased overall end-to-end latency.

2) *Network Air Interface:* The high density of connected devices to the 5G network will result in high interference. Advanced media access techniques, such as NOMA, have been introduced to mitigate this issue [38], which allows multiple users to access the 5G network simultaneously utilizing the same frequency resource while mitigating interference through successive interference cancelation (SIC). However, NOMA requires addressing several limitations and implementation challenges, including the need for users to decode all the users' data in the same cell before decoding their own data, leading to increased receiver complexity and higher energy consumption compared with orthogonal media access (OMA).

As previously mentioned, 5G is expected to utilize the mm-wave band due to the extended range of spectrum availability in this band. The wavelengths of mm-wave allow for implementing compact massive multiple input and multiple output (MIMO) antenna arrays suitable for CBS and UV. Massive MIMO antenna arrays can be used to provide substantial beamforming gains to counteract the high path loss at mm-wave frequencies, and spatial reuse can help reduce the interference [39], [40]. However, it is essential to note that NOMA, massive MIMO arrays, and beamforming techniques demand high computational and processing complexity, which presents a challenge for the UVs' batteries.

3) *Network Security:* 5G introduces a new trust model with security features to ensure verifiable and authenticated interactions between subscribers and the network. These features include interoperator security and privacy, primary and secondary authentication, key hierarchy, and radio network protection. This new trust model, along with its features, addresses the issues that plagued previous cellular network generations, which were based on the signaling system 7 [41] and diameter protocols [42]. However, the 5G network core will be built on software-defined networking (SDN) and network function virtualization (NFV) functionalities [43]. SDN and NFV heavily rely on the hypertext transfer protocol and representation state transfer application programmable interface (API) protocols [44], which are well known and widely used on the Internet. This reliance increases the risk of vulnerabilities and potential attacks on the 5G network.

With SDN and NFV being implemented for network slicing in 5G, network administration will become even more complex. The flexibility of 5G networks comes at the cost of increased complexity and the number of settings that require monitoring. This flexibility also means a higher likelihood of security configuration mistakes. Despite the presence of numerous security mechanisms in 5G networks, ensuring lasting security will necessitate unwavering commitment from telecom manufacturers and service providers responsible for standards implementation, as well as from the UAM operators themselves, who bear the responsibility for proper configuration and adherence to recommended practices.

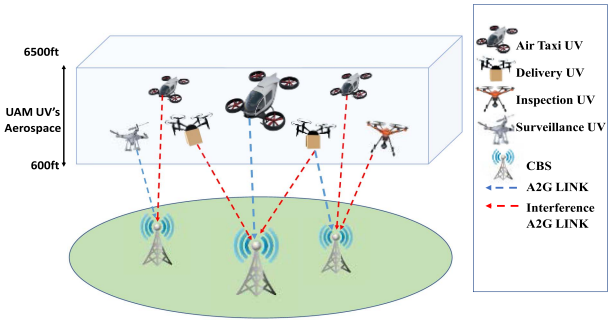

Fig. 2. Outline of the considered system model.

III. SYSTEM MODEL

The research presented in this article models a downlink network that focuses on the air-to-ground (A2G) communication between UVs and CBS considering the cochannel. The same analysis can be used for the uplink; however, in this article, we focused on the downlink channel. In UAM, the UAVs periodically send their surveillance information, such as their location and identification codes, to the ground station, similar to ADS-B. This information is crucial for separation assurance and collision avoidance (SA&CA) between UAVs.

Fig. 2 shows that the proposed system, which consists of UVs, deployed according to two scenarios: a random distribution following the homogeneous Poisson point process (PPP) distribution and a deterministic distribution following the grid model. The transmit power of all UVs is assumed to be fixed with mean $(1/\mu)$. The dense urban environment is considered; therefore, the channel is affected by Rayleigh fading due to the non-line-of-sight (NLOS) condition. The received power of a CBS at a distance r from the nearest UV is $h \cdot \mathrm{PL}^{-1}$, where h is a random variable of an exponential distribution with mean $(1/\mu)$ and PL is the path loss. The interference power is assumed to follow an exponential distribution g. The interference power at the CBS I_r is the received power summation of all other UVs except the nearest to the CBS. The noise power is considered additive and remains constant with a value of σ^2.

A. Path Loss Model

A stretched exponential path loss (SEPL) is proposed for the A2G channel because it accurately addresses the propagation in the dense urban environment [45]. Also, it helps to derive the network key metrics SINR and P_c in simple forms. The proposed SEPL is derived based on the A2G path loss in [46], which is proposed for dense urban environments and considers the line of sight (LOS) and the NLOS conditions. The path loss is expressed by

$$\mathrm{PL}_{A2G_{\mathrm{dB}}} = \mathrm{FSPL}_{\mathrm{dB}} + L_{a_{\mathrm{dB}}} + L_{d_{\mathrm{dB}}} + [(1 - P_{\mathrm{LOS}})]_{\mathrm{dB}}. \quad (1)$$

$\mathrm{FSPL}_{\mathrm{dB}}$ is the free-space path loss. This can be expressed as a function of ground distance and elevation angle as follows:

$$\mathrm{FSPL} = 20\log(r) - 20\log(\cos\theta) + 20\log(f) - 147.55 \tag{2}$$

where r is the ground distance (m), f is the frequency (Hz), θ is the elevation angle (°), and L_a is the antenna loss. For an omnidirectional antenna, L_a is calculated as follows:

$$L_a = -2\,G_o \tag{3}$$

where G_o is the maximum gain (dBi) and $L_{d\,\mathrm{dB}}$ is the excess path loss, which is given by

$$L_{d_{\mathrm{dB}}} = -68.8 + 10\log(f) + 10\log(h_B - h_{\mathrm{ms}}) + 20\log(\cos\theta) - 10\log\left(1 + \frac{\sqrt{2}}{L_r^2}\right). \tag{4}$$

Here, h_B is the building height (m), h_{ms} is the mobile station height (m), and L_r is the reflection coefficient (percent). The probability of LOS [47], [48] is given by

$$P_{\mathrm{LOS}}(r,\ h) = e^{\left(-2r_b\lambda_b\int_0^{r-\frac{\pi}{2}r_b} G(h)dx\right)} \tag{5}$$

where $G(h)$ is the complementary cumulative distribution of building height, r_b is the mean building radius in (m), and λ_b is the density of buildings in (buildings/m^2).

Considering a Rayleigh distribution $G(h) = e^{\left(-\frac{h_{\mathrm{UAV}}{}^2 x^2}{2\sigma_b{}^2 r^2}\right)}$ with $\sigma_b = \mu_b\sqrt{2/\pi}$, the probability of LOS can be modeled as follows:

$$P_{\mathrm{LOS}}(r,\ h) = e^{(-\beta r)} \tag{6}$$

where

$$\beta = \frac{2r_b\lambda_b\mu_b}{h_{\mathrm{UAV}}}\left[\phi\left(\frac{h_{\mathrm{UAV}}}{2\mu_b/\sqrt{\pi}}\right)\right]. \tag{7}$$

The total path loss (TPL) in dB is given by

$$\mathrm{PL}_{A2G_{\mathrm{dB}}} = A + 20\log(r) + 10\log\left[\left(1 - e^{(-\beta r)}\right)\right] \tag{8}$$

where the subfunction A is

$$A = -216.4 + 30\log(f) + 10\log(h_B - h_{\mathrm{ms}}) - 2G_o - 10\log\left(1 + \frac{\sqrt{2}}{L_r^2}\right). \tag{9}$$

The TPL can also be expressed in power ratio form as follows:

$$\mathrm{PL}_{A2G} = C\,r^2\left[1 - e^{(-\beta r)}\right] \tag{10}$$

where $C = 10^{\frac{A}{10}}$.

B. Probability of Coverage

The PoC (P_c) is defined as the probability of a UV being connected to the nearest CBS, which can be expressed by

$$P_c(T,\lambda) \triangleq P[\mathrm{SINR} > T] \tag{11}$$

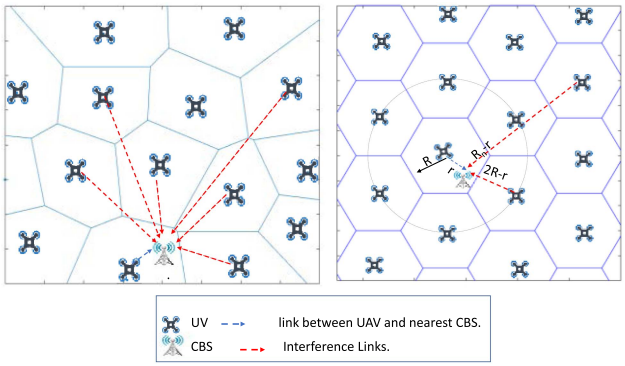

Fig. 3. (a) Top view of PPP distributed UAM network. (b) Top view of grid model for UAM network.

where T is the threshold SINR and ρ is the UVs density. A UV is connected by the nearest CBS when the SINR is larger than the threshold (T). The SINR can be expressed by

$$\mathrm{SINR} = \frac{P_{Rx}}{\sigma^2 + I_r} \tag{12}$$

where the received power is $P_{Rx} = hC^{-1}r^{-2}(1 - e^{-\beta r})^{-1}$; the interference power is $I_r = \sum gC^{-1}r^{-2}(1 - e^{-\beta r})^{-1}$; and σ^2 is the thermal noise.

The PoC is derived for two scenarios: a UAM network where UA is randomly placed according to a PPP distribution, and a grid network whose UVs are uniformly distributed, as shown in Fig. 3(a) and (b), respectively.

1) *Probability of Coverage for PPP Distribution:* Fig. 3(a) shows a UAM network where UA is randomly placed according to a PPP distribution. In the figure, Poc of a random UV in the network is

$$P_c(T,\ \lambda) = E_r\ [P[\mathrm{SINR} > T|r]]. \tag{13}$$

Based on the previous discussion, we can also write

$$P_c(T,\ \lambda) = \int_{r>0} P\left[\frac{hC^{-1}r^{-2}\left(1 - e^{(-\beta r)}\right)^{-1}}{\sigma^2 + I_r} > T|r\right] f_r(r)\,dr. \tag{14}$$

From [49], the probability density function (PDF) as a function of the distance between the CBS and the nearest UV (r) is

$$f_r(r) = \frac{df_r(r)}{dr} = 2\,\pi\,\lambda\,r\,e^{-\lambda\pi r^2}. \tag{15}$$

Then, the P_c can be expressed by

$$P_c(T,\lambda) = \int_0^{\infty} e^{-\lambda\pi y\left(T^{\frac{2}{3}}x(T)+1\right)} e^{\left(-\mu C\beta y^{3/2}T\sigma^2\right)}\pi\lambda\,dy \tag{16}$$

where

$$x(T) = \frac{\pi}{\sqrt{3}} - \frac{1}{3}\left[-2\ln\left(T^{\frac{-1}{3}} + 1\right) + -\ln\left(T^{\frac{-2}{3}} - T^{\frac{-1}{3}} + 1\right)\right]. \tag{17}$$

It should be noted that, in dense networks, σ^2 is very small compared with the desired signal power [50]. Therefore, PoC can be approximated by

$$P_c(T,\ \lambda) = \frac{1}{Z} - \frac{3\sqrt{\pi}\ \left(\pi\lambda\mu C\beta T\sigma^2\right)}{4(\lambda\pi Z)^{\frac{5}{2}}} \tag{18}$$

where $Z = T^{\frac{2}{3}}x(T) + 1$

For no noise ($\sigma^2 = 0$), PoC depends only on T. Therefore

$$P_c(T,\ \lambda) = P_c(T) = \frac{1}{T^{\frac{2}{3}}x(T) + 1}. \tag{19}$$

Appendix 1 presents the derivation of (16), (18), and (19).

2) *Probability of Coverage for the Grid Model:* The method described in [51] models the uniform grid network. This method calculates cumulative interference by substituting the actual network with an equivalent network in which UVs, with density ρ, are uniformly distributed. The served UV is assumed to be the origin of the polar coordinate plane, and r represents the distance between the aircraft and the CBS, as illustrated in Fig. 3(b). The distance between the CBS and the first circle of the interfered aircraft is $(2R - r)$, where R is the coverage radius of the served UV. The distance between CBS and the last circle of the interfered UVs is given by $(Rn - r)$.

Given that the coverage radius of a UV is R, the distance between two adjacent UVs is $2R$, where $R \propto 1/\sqrt{\rho}$. Therefore, cumulative interference can be approximated to [51]

$$I_r = \sum_{l=1}^{N_r} \int_0^{2\pi} \int_{2R-r+\varepsilon_l-1}^{2R-r+\varepsilon_l} h(C\beta)^{-1} r^{-3} \rho\ z\ dz\ d\theta. \tag{20}$$

The average of I_r is given by

$$E[I_r] = \frac{2\pi\rho\mu}{C\beta}\left[(2R - r)^{-1} - (R_n - r)^{-1}\right]. \tag{21}$$

The PoC is defined as follows:

$$P_c(T,\ \rho) = E_r\left[E_{Ir}\ \left[P\left\{\text{SINR} > T\right\}\right]\right] \tag{22}$$

where

$$\text{SINR} = \frac{P_{Rx}}{\sigma^2 + E[I_r]}. \tag{23}$$

The received power $(P_{Rx}) = hC^{-1}r^{-2}(1 - e^{(-\beta r)})^{-1}$ and the average cumulative interference can be approximated by $E[I_r] = \frac{2\pi\lambda\mu}{C\beta}(2R - r)^{-1}$, assuming that the network is widely expanded $R_n \to \infty$ and the term $(R_n - r)^{-1} \to 0$ (21). The PDF [51] of the distance r between the UV and the nearest CBS is

$$f(r) = \frac{2\ \rho}{c_{nm}^2} r, \qquad 0 \le r\ \le R \tag{24}$$

where $c_{nm}^2 = c_f^2$ is a normalized factor, $c_f^2 = 0.5$, $c_f^2 = {}^1\!/\!_{2\sqrt{3}}$, and $c_f^2 = {}^1\!/\!_{\pi}$ for square, hexagonal, and circle grids.

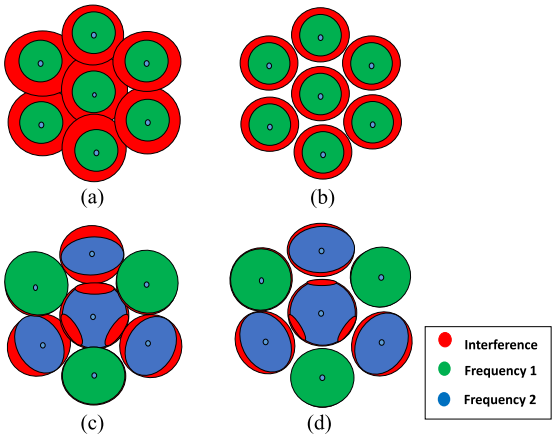

Fig. 4. (a) Initial interference. (b) Interference mitigation using SD. (c) Interference mitigation using FR, $\delta = 2$. (d) Interference mitigation using (FR-SD).

Then, the probability of coverage is expressed by

$$P_c(T,\ \rho) = \frac{1}{R^2}\int_0^{R^2} e^{-\mu T r^{\frac{3}{2}}\left(C\beta\sigma^2 + \frac{2\pi\rho\mu}{2R - r^{1/2}}\right)}\ dr,$$
$$\text{where } \rho = {}^{c_f^2}\!/\!_{R^2}. \tag{25}$$

When the thermal noise is neglected $\sigma^2 = 0$, the probability of coverage is reduced to

$$P_c(T,\ \rho) = \frac{1}{R^2}\int_0^{R^2} e^{\frac{-2\pi\rho\mu^2 T r^{3/2}}{(2R - r^{1/2})}}\ dr. \tag{26}$$

IV. PROBABILITY OF COVERAGE ENHANCEMENT

The PoC can be improved by mitigating the cochannel interference. The interference management techniques were proposed in [18], [19], [22], [52], [53], and [54]. The CIC strategies were proposed in [18], [19], and [52]. A DF method for multibeam UAV to avoid cochannel interference was proposed in [40] and [52]. In [19], a QF-based CIC method for uplink communication was presented. Liu et al. [53] proposed the coordinate multipoint architecture for multi-UAV to mitigate interference. In [54], the cooperative NOMA was proposed to avoid uplink interference. The NOMA algorithm to reduce cochannel interference for cellular-connected UAV was presented in [22]. However, these techniques require high processing power, which increases the power consumption of the UAVs battery. Therefore, we propose a combined method using both FR and SD in order to improve PoC while also reducing cochannel interference. This combined FR-SD method also requires lower processing power compared with the other methods mentioned above. In the SD method, the interference is reduced by decreasing the UV coverage radius and setting a separation distance *(d)* between the coverage area of UV, as shown in Fig. 4(b). The increase in PoC is due to the inverse proportional relation between PoC and the square of coverage radius R^2 from (26). In the FR method, PoC increased by employing FR, where the network utilizes different frequency bands. Here, δ, with $\delta \ge 1$, determines

the number of frequencies being used. The density of interfering UVs that transmit in the same frequency band is reduced to ρ/δ, as shown in Fig. 4(c). Subsequently, for the PPP model, the PoC in (16) can be expressed by

$$P_c\,(T,\lambda,\delta) \;=\; \int_0^{\infty} e^{-\lambda\pi y\left(\frac{T^{\frac{2}{\delta}}x(T)}{\delta}+1\right)} e^{\left(-\mu C\beta y^{3/2}T\sigma^2\right)}\pi\lambda\, dy. \tag{27}$$

Neglecting thermal noise ($\sigma \;=\; 0$), the PoC is

$$P_c\,(T,\;\delta) = \frac{1}{\frac{T^{\frac{2}{\delta}}x(T)}{\delta}+1}. \tag{28}$$

For the grid model, the PoC in (25) can be expressed by

$$P_c\,(T,\;\lambda) = \frac{1}{R^2}\int_0^{R^2} e^{-\mu T r^{\frac{3}{2}}\left(P^{-1}\sigma^2+\frac{2\pi\rho\mu T r^{\frac{3}{2}}}{\left(2R-r^{1/2}\right)\delta}\right)}\, dr. \tag{29}$$

Neglecting thermal ($\sigma = 0$), the PoC is

$$P_c\,(T,\;\lambda) = \frac{1}{R^2}\int_0^{R^2} e^{\frac{-2\pi\rho\mu T r^{3/2}}{\left(2R-r^{1/3}\right)\delta}}\, dr. \tag{30}$$

The combined FR-SD method increases the coverage area by a factor δ compared with the SD method and saves frequency resources compared with the FR method, as shown in Fig. 4(d). The increase in the coverage associated with the new coverage radius (R_{new}), which can be obtained as follows:

$$R_{\text{new}} = \sqrt{c_f^2\Big/\left(\frac{\rho}{\delta}\right)} = R\sqrt{\delta}. \tag{31}$$

Therefore, the coverage area is increased by a factor $\delta = \frac{R_{\text{new}}^2}{R^2}$.

A. FR-SD Algorithm

The proposed algorithm uses the FR-SD method to maximize the PoC of the deployed UV. First, the maximum allowable path loss (PL_{th}) is calculated by

$$\text{PL}_{\text{th}} \;=\; P_{\text{UV}_{Tx}} \;-\; P_{\text{CBS}_{Rx}}\;. \tag{32}$$

Then, the coverage radius of a single UV is calculated from the path loss (10). The number of UV in the network area is calculated by

$$N = \frac{C_f^2 \;\cdot\; \text{Total Network Area}}{R^2},\; N_{\text{int}} = \text{round}\,(N)\,. \tag{33}$$

The density of the UV network is calculated by

$$\lambda = \frac{N_{\text{int}}}{\text{Total Network Area}}. \tag{34}$$

Then, the PoC is calculated using the grid model, which gives the optimistic P_c. Then, the PPP model is used to calculate the pessimistic P_c. The actual P_c is assumed to be the average of the PPP model and the grid model results. The algorithm increments δ till its limit. If the P_c does not achieve the target value (P_{c_th}), then it will begin to increase the separation distance until it reaches the target P_c.

(FR-SD) Algorithm: FR-SD Method–Iterative Algorithm.

Inputs: (h_{MS}, G_o, L_r, α_3, h_B, f, $P_{\text{UAV}_{Tx}}$, $P_{\text{TUAV}_{Rx}}$, $P_{\text{MS}_{Rx}}$, T, P_{c_th})
Outputs: (δ, R, N, P_c)
1 Obtain R_{int} for single UV
2 Obtain N number of UV
3 Obtain $\boldsymbol{\lambda}$
4 Set $\delta = 1$ and $d = 0$
5 Calculate P_c for grid network @ T and λ
while ($P_c < P_{c\_\text{th}}$ AND $\delta < \delta$ _th) do
    $\delta = \delta{+}1$
Then, recalculate P_c
while ($P_c < P_{c\_\text{th}}$) do
    $R{=}R_{\text{int}}{-}1$
    $d = 2{*}(d{+}1)$
Then, recalculate P_c

TABLE II
Network Parameters [57]

Parameter	Value
Network Area	4 km^2
Frequency (f)	2 GHz
$\boldsymbol{PL_{th}}$	120 dBm
SINR	From −10 to 20 dB

B. Computational Complexity

The proposed FR-SD method is based on OMA technology, while the other methods are based on NOMA [18], [19], [22], [52], [53], [54]. In NOMA, the implementation of real-time power allocation and SIC algorithms demands significant computational power [55]. For instance, with M possible modulation orders and K subcarriers, the total number of combinations required to determine the optimal modulation orders for N OMA users is $N \cdot M^K$ [56]. For NOMA, it is necessary to load the subcarriers of all users simultaneously, resulting in a total of M^{KN} combinations [56], which is substantially more significant than the OMA case.

V. NUMERICAL RESULTS AND DISCUSSION

In this section, MATLAB Monte Carlo simulation is employed to validate the theoretical analysis. Subsequently, the impact of noise is investigated. Following that, a comparison among SD, RF, and RF-SD methods is presented, followed by a discussion of the results. The simulation parameters are chosen to reflect the urban network parameters proposed in [50], where the network area is 4 km^2, and the operating frequency is 2 GHz. The maximum allowable path loss between UV and CBS is set at 120 dBm, with an SINR threshold range from −10 to 20 dB. The network parameters are listed in Table II.

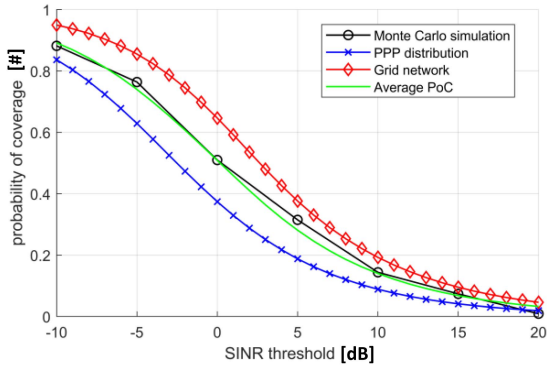

Fig. 5. Theoretical models versus Monte Carlo simulation.

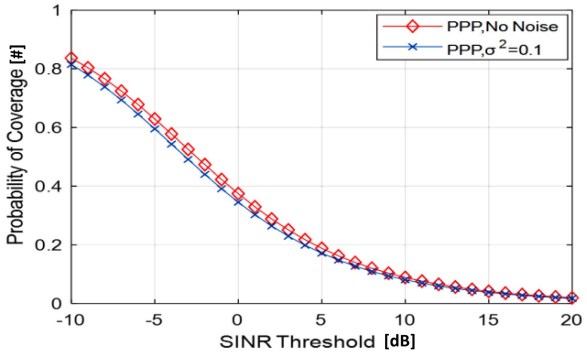

Fig. 6. P_c versus SINR threshold.

A. Theoretical Models Versus Simulation

The comparison between the theoretical models and the Monte Carlo simulation is illustrated in Fig. 5. The grid network exhibits a higher PoC compared with the simulation, while the PoC of the PPP network is lower than that in the simulation. This difference can be explained by analyzing the specificities of the two models. In the grid model, the distance between a certain UV and the other interfering UV is not closer than $2R$, where R is the coverage radius of the aircraft. This condition is more idealized than the real network. In the PPP model, the distance between UVs is randomly distributed, allowing both serving and interfering UVs to be close to the CBS, resulting in more interference power than in the real network. Therefore, the PPP model provides more pessimistic results due to the strong interference generated by nearby UVs. On the other hand, the grid model is more optimistic because actual UV networks always exhibit a certain degree of irregularity. The actual PoC is the average of the grid and PPP networks, validated by the Monte Carlo simulation, which aligns with the average PoC, as depicted in Fig. 5.

B. Effect of Thermal Noise on the Probability of Coverage

Fig. 6 shows the PoC versus SINR for $\sigma^2 = 0.1$ and $\sigma^2 = 0$ (no-noise). A difference of less than 1 dB gap is observed between the two cases. Therefore, the noise can be neglected in dense networks as they are interference-limited networks, as explained in [50].

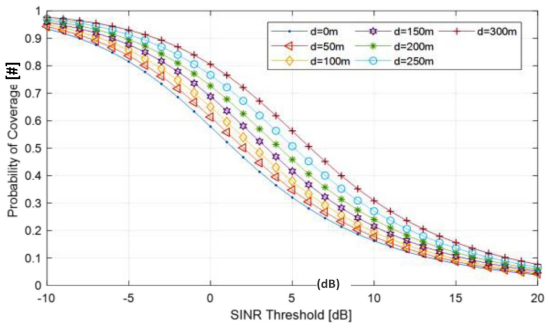

Fig. 7. P_c versus SINR at different separation distances.

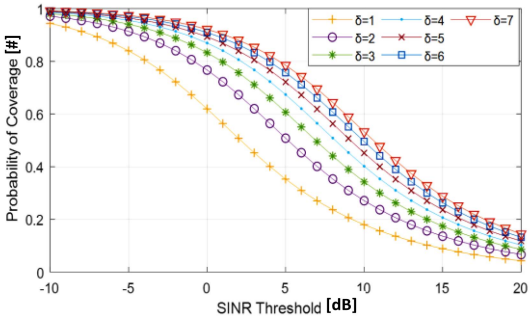

Fig. 8. P_c versus SINR at different FRs.

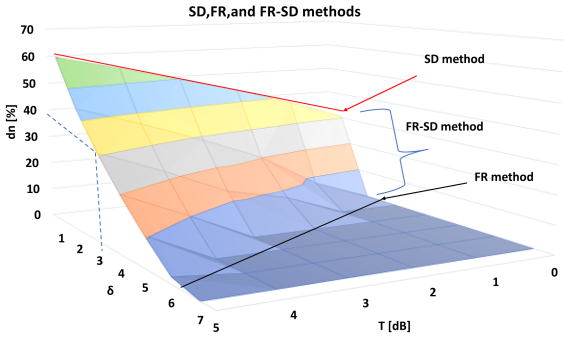

Fig. 9. SD, FR, and FR-SD methods versus δ, dn, and T.

C. Comparing SD, FR, and FR-SD Methods

Using SD method, the PoC increases from 0.6 to 0.8 at $T = 0$ and $d = 300$ m, as shown in Fig. 7, while by using FR method, the PoC increases from 0.6 to 0.92 at $T = 0$ and $\delta = 7$, as shown in Fig. 8. Fig. 9 shows the FR-SD method, SD method, and FR method versus δ and the normalized separation distance with respect to coverage radius (dn) for different values of T. For a PoC of 0.8 and $\delta = 3$, the proposed algorithm improves the coverage area by a factor 3 compared with the SD method. Also, it saves the frequency resources by a factor 3 compared with the FR method [58], [59], [60].

D. Discussion of Results

The envisioned UAM operational context will be characterized by a vast variety of missions and vehicles, ranging from very light hovering inspection platforms to medium-class point-to-point air taxis carrying multiple passengers. In this context, ever-changing UV densities and the highly

variable throughput requirements associated with their missions will require a flexible approach to assure a minimum acceptable level of communication performance (and, therefore, operational safety). The benefits of combining the complementary advantages of FR and SD are compelling in the given scenario and this was corroborated by our simulation results, where the tradeoff between the two baseline methods allows to achieve the best compromise of threshold SINR, coverage factor, and normalized separation distance. For instance, the already significant gains in PoC achievable by increasing the coverage factor to just 3 can be compounded with the PoC gains achieved by a reasonable increase in the minimum separation distance between terminals, which can be stipulated as a part of the UAM SA&CA requirements, as in the case of the unified SA&CA methodology proposed in the previous research. Doing so allows the FR-SD approach to easily achieve very high PoC while also minimizing the energy consumption of the cellular communication system onboard the UV by not relying less heavily on NOMA, massive MIMO, and beamforming functionalities.

VI. CONCLUSION

UAM aims to provide a safe and efficient air transportation mode for people and goods in urban areas. UAM encounters crucial challenges encompassing UV design, aerodromes implementation, and manned/unmanned air traffic management. The commercial viability of UAM will require reliable broadband A2G communications between aircraft and ground terminals to optimally utilize the airspace resources and to create a safe, efficient, and sustainable transportation system. In this article, the potential of UAM communication systems using state-of-the-art cellular network technology was discussed in detail and a wireless connectivity performance analysis was carried out, which specifically addressed cochannel interference between UV and CBS, which is one of the most important challenges arising in dense UAM operations. Using stochastic geometry, mathematical expressions for the PoC were derived and used to analyze the PoC enhancement provided by interference mitigation techniques, such as FR and SD. A PoC enhancement algorithm using the combined FR-SD method was proposed. Simulation results corroborate the potential benefits of this combined approach by achieving significant gains in PoC with limited increases in coverage factor and minimum separation distance, which can be stipulated as a part of the SA&CA requirements. The FR-SD approach also allows minimizing the energy consumption of the cellular communication system onboard the UV by relying less heavily on power-intensive computational functionalities as NOMA, massive MIMO, and beamforming. The FR-SD method ideally fits the unified SA&CA methodology that was proposed in the previous research, as this unified mathematical approach allows for a continuously evolving separation volume based on the achievable CNS performance, which can be augmented locally by infrastructure or temporary relays, such as HAP, TUAV, and other LAP, which were briefly discussed in this article. Further research shall investigate the integration of the unified SA&CA methodology with the FR-SD method and the optimal local augmentation approach for communication performance in the densest UAM traffic conditions.

ACKNOWLEDGMENT

The authors would like to thank Khalifa University (Abu Dhabi, UAE) for supporting this work through the Grant No. FSU-2022-013.

APPENDIX

The P_c of a random UV in the network is

$$P_c(T,\ \lambda) = E_r\ [P[\text{SINR} > T|r]] \tag{35}$$

$$= \int_{r>0} P\left[\frac{hC^{-1}\mathrm{r}^{-2}\left(1-e^{(-\beta r)}\right)^{-1}}{\sigma^2+I_r} > T|r\right] f_r(r)\,dr \tag{36}$$

where $f_r(r)$ is the PDF of the distance r between CBS and the closet UV, which is expressed as follows:

$$f_r(r) = \frac{df_r(r)}{dr} = 2\pi\lambda r\, e^{-\lambda\pi r^2} \tag{37}$$

$$P_c(T,\ \lambda) = \int_{r>0} P\left[\frac{hC^{-1}r^{-2}\left(1-e^{-\beta r}\right)^{-1}}{\sigma^2+I_r} > T|r\right] 2\pi\lambda r e^{-\lambda\pi r^2} dr \tag{38}$$

where

$$P\left[\frac{hC^{-1}r^{-2}\left(1-e^{-\beta r}\right)^{-1}}{\sigma^2+I_r} > T|r\right]$$

$$= P\left[h > Cr^2\left(1-e^{-\beta r}\right)\ T\left(\sigma^2+I_r\right)|r\right] \tag{39}$$

$$=\ E_{Ir}\left[-\mu Cr^2\left(1-e^{-\beta r}\right)T\left(\sigma^2+I_r\right)|r\right] \tag{40}$$

$$= e^{\left[-\mu Cr^2\left(1-e^{-\beta r}\right)T\sigma^2\right]}\ L_{Ir}\left[\mu TCr^2\left(1-e^{-\beta r}\right)\right] \tag{41}$$

$$P_c(T,\lambda) = \int_{r>0} e^{-\lambda\pi r^2} e^{-\mu Cr^2\left(1-e^{-\beta r}\right)T\sigma^2} \cdot\left[\mu TCr^2\left(1-e^{-\beta r}\right)\right] 2\pi\lambda r dr. \tag{42}$$

Applying the Laplace transform results in

$$L_{Ir}(s) = E_{Ir}\left[e^{-sI_r}\right] \tag{43}$$

$$= E_{\phi,g_i}\left[e^{-s\sum g_i C^{-1}R_i^{-2}\left(1-e^{-\beta R_i}\right)^{-1}}\right] \tag{44}$$

$$= E_{\phi,g_i}\left[\Pi e^{-sg_iC^{-1}R_i^{-2}}\left(1-e^{-\beta R_i}\right)^{-1}\right] \tag{45}$$

$$= e^{-2\pi\lambda\int_r^\infty\left[1-\int_0^\infty \mu e^{-(s\Psi+\mu)g}dg\right]vdv} \tag{46}$$

where

$$\Psi = e^{e^{-sC^{-1}v^{-2}\left(1-e^{-\beta v}\right)^{-1}}}. \tag{47}$$

Then, (46) can be expressed by

$$L_{Ir}(s) = e^{-2\pi\lambda\int_r^\infty\left[1-\frac{\mu}{\mu+\Psi}\right]vdv}. \tag{48}$$

Replacing s with $\mu\, C\, r^2(1-e^{-\beta r})$ and substituting (47) in (48)

$$L_{Ir}\left(\mu C r^2\left(1-e^{-\beta r}\right)\right) = e^{-2\pi\lambda\int_r^\infty \left[1-\frac{\mu}{\mu+\mu T\left(r/v\right)^2\left(\frac{1-e^{(-\beta r)}}{1-e^{(-\beta v)}}\right)}\right] v dv}. \quad (49)$$

For dense urban, $\beta = 1.4\cdot 10^{-3}$ at a UV height of 600 m. Therefore, $1-e^{(-\beta r)}$ can be approximated to βr. Therefore, (49) is approximated to

$$L_{Ir}\left(\mu TC\beta r^3\right) = e^{-2\pi\lambda\int_r^\infty \frac{1}{1+T^{-1}\,(t/v)^3}\, v dv}. \quad (50)$$

By changing the variables $(v/r)^3\cdot T^{-1} = U^{3/2}$.

$$L_{Ir}\left(\mu TC\beta r^3\right) = e^{-\pi\lambda T^{2/3} r^2\int_{T^{-2/3}}^\infty \frac{1}{1+U^{3/2}}\, dU} \quad (51)$$

$$L_{Ir}\left(\mu TC\beta r^3\right) = e^{-\pi\lambda T^{\frac{2}{3}} r^2 x(T)} \quad (52)$$

where

$$x(T) = \frac{\pi}{\sqrt{3}} - \left[1/3\left(-2\ln\left(T^{-1/3}+1\right) + \ln\left(T^{-2/3}-T^{-1/3}+1\right)\right)\right] \quad (53)$$

$$P_c(T,\lambda) = \int_0^\infty e^{-\lambda\pi r^2\left(T^{\frac{2}{3}}x(T)+1\right)} e^{\left(-\mu C\beta r^3 T\sigma^2\right)} 2\pi\lambda r dr. \quad (54)$$

By changing variable $r^2 = y$

$$P_c(T,\lambda) = \int_0^\infty e^{-\lambda\pi y\left(T^{\frac{2}{3}}x(T)+1\right)} e^{\left(-\mu C\beta y^{3/2} T\sigma^2\right)} \pi\lambda\, dy. \quad (55)$$

For $\sigma^2 =$ small value

$$e^{\left(-\mu C\beta y^{3/2}T\sigma^2\right)} \approx 1-\mu C\beta y^{3/2} T\sigma^2 \quad (56)$$

$$P_c(T,\lambda) = \int_0^\infty e^{-\lambda\pi y\left(T^{\frac{2}{3}}x(T)+1\right)}\left(1-\mu C\beta y^{\frac{3}{2}} T\sigma^2\right)\pi\lambda\, dy \quad (57)$$

$$P_c(T) = \frac{1}{T^{\frac{2}{3}}x(T)+1} - \left(\pi\lambda\mu C\beta T\sigma^2\right)\int_0^\infty e^{-\lambda\pi y\left(T^{\frac{2}{3}}x(T)+1\right)} y^{\frac{3}{2}}\, dy \quad (58)$$

$$\int_0^\infty e^{-\lambda\pi Z y} y^{\frac{3}{2}}\, dy = \left.\frac{3\sqrt{\pi}\; erf\left(\sqrt{\lambda\pi Z}\sqrt{y}\right)}{4(\lambda\pi Z)^{\frac{5}{2}}}\right|_0^\infty - \left.\frac{\sqrt{y}e^{-\lambda\pi Z y}\left(2y\lambda\pi Z+3\right)}{2(\lambda\pi Z)^2}\right|_0^\infty \quad (59)$$

$$P_c(T,\lambda) = \frac{1}{Z} - \frac{3\sqrt{\pi}\left(\pi\lambda\mu C\beta T\sigma^2\right)}{4(\lambda\pi Z)^{\frac{5}{2}}},$$

where $Z = \left(T^{\frac{2}{3}}x(T)+1\right)$. (60)

REFERENCES

[1] K. Messaoudi, O. S. Oubbati, A. Rachedi, A. Lakas, T. Bendouma, and N. Chaib, "A survey of UAV-based data collection: Challenges, solutions and future perspectives," *J. Netw. Comput. Appl.*, vol. 216, 2023, Art. no. 103670.

[2] B. Alzahrani, O. S. Oubbati, A. Barnawi, M. Atiquzzaman, and D. Alghazzawi, "UAV assistance paradigm: State-of-the-art in applications and challenges," *J. Netw. Comput. Appl.*, vol. 166, 2020, Art. no. 102706.

[3] R. Sabatini et al., "Avionics systems panel research and innovation perspectives," *IEEE Aerosp. Electron. Syst. Mag.*, vol. 35, no. 12, pp. 58–72, Dec. 2020.

[4] P. Fontaine, "Urban air mobility (UAM) concept of operations V2.0," Federal Aviation Administ., Washington, DC, USA, 2023. Accessed: Apr. 26, 2023.

[5] S. Bradford, "Urban air mobility (UAM) concept of operations," , Federal Aviation Administ., Washington, DC, USA, 2020. Accessed: Jul. 15, 2020.

[6] N. Pongsakornsathien et al., "A performance-based airspace model for unmanned aircraft systems traffic management," *Aerospace*, vol. 7, no. 11, 2020, Art. no. 154.

[7] LLP Deloitte Consulting, "UAM vision concept of operations (CONOPS) UAM maturity level (UML) 4," Document ID 20205011091, NASA, NTRS–NASA Tech. Rep. Server, London, U.K., 2020.

[8] S. Whiteside and B. Pollard, "Conceptual design of a tiltduct reference vehicle for urban air mobility," in *Proc. Aeromech. Adv. Vertical Flight Tech. Meeting*, 2022.

[9] S. Whiteside et al., "Design of a tiltwing concept vehicle for urban air mobility," NASA/TM-20210017971, 2021.

[10] W. Johnson, "A quiet helicopter for air taxi operations," in *Proc. Aeromech. Adv. Vertical Flight Tech. Meeting*, ARC-E-DAA-641TN76202, 2020.

[11] M. Radotich, "Conceptual design of two tiltrotor aircraft for urban air mobility," Univ. of Alaska Fairbanks, Fairbanks, AK, USA, 2021.

[12] A. Gardi, R. Sabatini, and T. Kistan, "Multiobjective 4D trajectory optimization for integrated avionics and air traffic management systems," *IEEE Trans. Aerosp. Electron. Syst.*, vol. 55, no. 1, pp. 170–181, Feb. 2019.

[13] R. Sabatini, T. Moore, and S. Ramasamy, "Global navigation satellite systems performance analysis and augmentation strategies in aviation," *Prog. Aerosp. Sci.*, vol. 95, pp. 45–98, 2017.

[14] S. Bijjahalli, R. Sabatini, and A. Gardi, "GNSS performance modelling and augmentation for urban air mobility," *Sensors*, vol. 19, no. 19, 2019, Art. no. 4209.

[15] M. Series, "Reception of automatic dependent surveillance broadcast via satellite and compatibility studies with incumbent systems in the frequency band 1 087.7-1 092.3 MHz." *Int. Telecommun. Union*, Geneva, Switzerland, 2017.

[16] Y. Pan et al., "When UAVs coexist with manned airplanes: Large-scale aerial network management using ADS-B," *Trans. Emerg. Telecommun. Technol.*, vol. 30, no. 10, 2019, Art. no. e3714.

[17] T. Zeng, O. Semiari, W. Saad, and M. Bennis, "Wireless-enabled asynchronous federated Fourier neural network for turbulence prediction in urban air mobility (UAM)," *IEEE Trans. Wireless Commun.*, vol. 22, no. 11, pp. 7902–7916, Nov. 2023.

[18] L. Liu, S. Zhang, and R. Zhang, "Multi-beam UAV communication in cellular uplink: Cooperative interference cancellation and sum-rate maximization," *IEEE Trans. Wireless Commun.*, vol. 18, no. 10, pp. 4679–4691, Oct. 2019.

[19] W. Mei and R. Zhang, "Uplink cooperative interference cancellation for cellular-connected UAV: A quantize-and-forward approach," *IEEE Wireless Commun. Lett.*, vol. 9, no. 9, pp. 1567–1571, Sep. 2020.

[20] J. Lu, J. Li, F. R. Yu, W. Jiang, and W. Feng, "UAV-assisted heterogeneous cloud radio access network with comprehensive interference management," *IEEE Trans. Veh. Technol.*, vol. 73, no. 1, pp. 843–859, Jan. 2024.

[21] Y. Kwon, H. Baek, and J. Lim, "Uplink NOMA using power allocation for UAV-aided CSMA/CA networks," *IEEE Syst. J.*, vol. 15, no. 2, pp. 2378–2381, Jun. 2020.

[22] R. Jain, A. Trivedi, and A. Gupta, "Co-channel interference suppression for cellular-connected UAV using NOMA," in *Proc. IEEE 4th Conf. Inf. Commun. Technol.*, 2020, pp. 1–6.
[23] O. S. Oubbati, M. Atiquzzaman, H. Lim, A. Rachedi, and A. Lakas, "Synchronizing UAV teams for timely data collection and energy transfer by deep reinforcement learning," *IEEE Trans. Veh. Technol.*, vol. 71, no. 6, pp. 6682–6697, Jun. 2022.
[24] A. S. Abdalla and V. Marojevic, "Communications standards for unmanned aircraft systems: The 3GPP perspective and research drivers," *IEEE Commun. Standards Mag.*, vol. 5, no. 1, pp. 70–77, Mar. 2021.
[25] A. Baltaci, E. Dinc, M. Ozger, A. Alabbasi, C. Cavdar, and D. Schupke, "A survey of wireless networks for future aerial communications (FACOM)," *IEEE Commun. Surv. Tut.*, vol. 23, no. 4, pp. 2833–2884, Oct.–Dec. 2021.
[26] A. A. Zaid, B. E. Y. Belmekki, and M. S. Alouini, "eVTOL communications and networking in UAM: Requirements, key enablers, and challenges," *IEEE Commun. Mag.*, vol. 61, no. 8, pp. 154–160, Aug. 2023.
[27] Int. Telecommun. Union, "Requirements for communication services of civilian unmanned aerial vehicles," Recommendation ITU-T F.749.10, Geneva, Switzerland, 2019.
[28] R. Shrestha, R. Bajracharya, and S. Kim, "6G enabled unmanned aerial vehicle traffic management: A perspective," *IEEE Access*, vol. 9, pp. 91119–91136, 2021.
[29] E. M. Mohamed, "Deployment of mmWave multi-UAV mounted RISs using budget constraint Thompson sampling with collision avoidance," *ICT Express*, vol. 10, no. 2, pp. 277–284, 2024, doi: 10.1016/j.icte.2023.07.011.
[30] S. Alraih et al., "Revolution or evolution? Technical requirements and considerations towards 6G mobile communications," *Sensors*, vol. 22, no. 3, 2022, Art. no. 762.
[31] W. Jiang, B. Han, M. A. Habibi, and H. D. Schotten, "The road towards 6G: A comprehensive survey," *IEEE Open J. Commun. Soc.*, vol. 2, pp. 334–366, Feb. 2021.
[32] I. F. Akyildiz, A. Kak, and S. Nie, "6G and beyond: The future of wireless communications systems," *IEEE Access*, vol. 8, pp. 133995–134030, 2020.
[33] L. Chen, M. A. Kishk, and M. S. Alouini, "Dedicating cellular infrastructure for aerial users: Advantages and potential impact on ground users," *IEEE Trans. Wireless Commun.*, vol. 22, no. 4, pp. 2523–2535, Apr. 2022.
[34] F. Gao, W. Su, R. Shan, W. Zhu, K. He, and L. Wang, "3D coverage optimization research on 5G massive MIMO antenna array," in *Proc. IEEE Int. Symp. Electromagn. Compat./IEEE Asia-Pacific Symp. Electromagn. Compat.*, 2018, pp. 94–97.
[35] S. Zhang, "An overview of network slicing for 5G," *IEEE Wireless Commun.*, vol. 26, no. 3, pp. 111–117, Jun. 2019.
[36] N. E. D. Safwat, M. H. Ismail, and N. Fatma, "3D placement of a new tethered UAV to UAV relay system for coverage maximization," *Electronics*, vol. 3, 2022, Art. no. 385.
[37] Radio Tech. Commission Aeronaut., "Command and control (C2) data link minimum operational performance standards (MOPS)(terrestrial), RTCA, incorporated," SC-228, Washington, DC, USA, 2016.
[38] T. M. Hoang, B. C. Nguyen, and T. Kim, "Outage and throughput analysis of UAV-assisted NOMA relay systems with indoor and outdoor users," *IEEE Trans. Aerosp. Electron. Syst.*, vol. 59, no. 3, pp. 2633–2647, Jun. 2023.
[39] A. F. Molisch et al., "Hybrid beamforming for massive MIMO: A survey," *IEEE Commun. Mag.*, vol. 55, no. 9, pp. 134–141, Sep. 2017.
[40] F. Rinaldi, A. Tropeano, S. Pizzi, A. Molinaro, and G. Araniti, "Dynamic MBSFN beam area formation in 6G multibeam non-terrestrial networks," *IEEE Trans. Aerosp. Electron. Syst.*, vol. 58, no. 5, pp. 3660–3774, Oct. 2022.
[41] K. Ullah, I. Rashid, H. Afzal, M. M. W. Iqbal, Y. A. Bangash, and H. Abbas, "SS7 vulnerabilities—A survey and implementation of machine learning vs rule based filtering for detection of SS7 network attacks," *IEEE Commun. Surv. Tut.*, vol. 22, no. 2, pp. 1337–1371, Oct. 2020.
[42] H. Tschofenig, D. Sebastien, M. Jean, and K. Jouni, *Diameter: New Generation AAA Protocol-Design, Practice, and Applications*. Hoboken, NJ, USA: Wiley, 2019.
[43] C. Bouras, A. Kollia, and A. Papazois, "SDN & NFV in 5G: Advancements and challenges," in *Proc. 20th Conf. Innov. Clouds, Internet Netw.*, 2017, pp. 107–111.
[44] N. Wehbe, A. A. Hyame, P. Makan, B. H. Elias, and A. Chadi, "A security assessment of HTTP/2 usage in 5G service-based architecture," *IEEE Commun. Mag.*, vol. 61, no. 1, pp. 48–54, Jan. 2023.
[45] A. AlAmmouri, J. G. Andrews, and F. Baccelli, "SINR and throughput of dense cellular networks with stretched exponential path loss," *IEEE Trans. Wireless Commun.*, vol. 17, no. 2, pp. 1147–1160, Feb. 2018.
[46] N. E.-D. Safwat, F. Newagy, and I. M. Hafez, "Air-to-ground channel model for UAVs in dense urban environments," *IET Commun.*, vol. 14, no. 6, pp. 1016–1021, 2020.
[47] A. Al-Hourani, "On the probability of line-of-sight in urban environments," *IEEE Wireless Commun. Lett.*, vol. 9, no. 8, pp. 1178–1181, Aug. 2020.
[48] A. Al-Hourani, "Interference modeling in low-altitude unmanned aerial vehicles," *IEEE Wireless Commun. Lett.*, vol. 9, no. 11, pp. 1952–1955, Nov. 2020.
[49] J. G. Andrews, F. Baccelli, and R. K. Ganti, "A tractable approach to coverage and rate in cellular networks," *IEEE Trans. Commun.*, vol. 59, no. 11, pp. 3122–3134, Nov. 2011.
[50] LTE Enhancing, "Cell-edge performance via PDCCH ICIC," pp. 1–16, 2011. [Online]. Available: http://www.fujitsu.com/downloads/TEL/fnc/whitepapers/Enhancing-LTE-Cell-Edge.pdf
[51] H. Zhang, S. Chen, L. Feng, Y. Xie, and L. Hanzo, "A universal approach to coverage probability and throughput analysis for cellular networks," *IEEE Trans. Veh. Technol.*, vol. 64, no. 9, pp. 4245–4256, Sep. 2015.
[52] L. Liu, S. Zhang, and R. Zhang, "Cooperative interference cancellation for multi-beam UAV uplink communication: A DoF analysis," in *Proc. IEEE Globecom Workshops*, 2018, pp. 1–6.
[53] L. Liu, S. Zhang, and R. Zhang, "CoMP in the sky: UAV placement and movement optimization for multi-user communications," *IEEE Trans. Commun.*, vol. 67, no. 8, pp. 5645–5658, Aug. 2019.
[54] W. Mei and R. Zhang, "Uplink cooperative NOMA for cellular-connected UAV," *IEEE J. Sel. Topics Signal Process.*, vol. 13, no. 3, pp. 644–656, Jun. 2019.
[55] W. U. Khan, G. A. S. Sidhu, X. Li, Z. Kaleem, and J. Liu, "NOMA-enabled wireless powered backscatter communications for secure and green IoT networks," in *Proc. Wireless-Powered Backscatter Commun. Internet Things*, 2021, pp. 103–131.
[56] T. Assaf, A. Al-Dweik, M. S. El Moursi, and H. Zeineldin, "Efficient bit loading algorithm for OFDM-NOMA systems with BER constraints," *IEEE Trans. Veh. Technol.*, vol. 71, no. 1, pp. 423–436, Jan. 2021.
[57] A. A. Khuwaja, G. Zheng, Y. Chen, and W. Feng, "Optimum deployment of multiple UAVs for coverage area maximization in the presence of co-channel interference," *IEEE Access*, vol. 7, pp. 85203–85212, 2019.
[58] C. Braithwaite and M. Scott, *UMTS Network Planning and Development: Design and Implementation of the 3G CDMA Infrastructure*. Amsterdam, The Netherlands: Elsevier, 2003.
[59] J. I. Agbinya, *Planning and Optimisation of 3G and 4G Wireless Networks*. Aalborg, Denmark: River Publishers, 2010.
[60] H. Tang, N. Yang, Z. Zhang, Z. Du, and J. Shen, *5G NR and Enhancements: From R15 to R16*. Amsterdam, The Netherlands: Elsevier, 2021.

Nour El-Din Safwat received the B.Sc., M.Sc., and Ph.D. degrees in electrical engineering from the Faculty of Engineering, Ain Shams University, Cairo, Egypt, in 2009, 2014, and 2022, respectively.

He is a Postdoctoral Fellow with the Department of Aerospace Engineering, Khalifa University of Science and Technology, Abu Dhabi, UAE. His research interests include wireless communications and UAV communications networks, urban air mobility, and UAS traffic management.

Roberto Sabatini received the Ph.D. degree in aerospace systems from Cranfield University, Cranfield, U.K., in 2004, and the Ph.D. degree in satellite navigation from the University of Nottingham, Nottingham, U.K., in 2017.

He is a Professor of aeronautics and astronautics with three decades of experience in Avionics, Spaceflight, and Robotics/ Autonomous Systems Research and Education. He holds other relevant academic/industrial qualifications in engineering and aviation disciplines, including the licenses of flight test engineer, private pilot, and remote pilot. His research addresses key contemporary challenges in aerospace systems design, test, and certification, with a focus on aircraft and spacecraft systems; guidance, navigation, and control; CNS/ATM systems; unmanned aircraft; intelligent vehicle health management; urban air mobility and UAS traffic management; and space domain awareness and space traffic management.

Alessandro Gardi received the B.Sc. and M.Sc. degrees in aerospace engineering from the Politecnico di Milano, Milan, Italy, in 2007 and 2011, respectively, and the Ph.D. degree in the same discipline from RMIT University, Melbourne, VIC, Australia, in 2017.

He is currently an Assistant Professor with Khalifa University, Abu Dhabi, UAE, and an Associate Professor with RMIT University, focusing on aerospace cyber-physical systems (UAS, satellites, ATM systems, and avionics). In this domain, he specializes in multiobjective trajectory optimization with an emphasis on optimal control methods, multidisciplinary design optimization, and AI/metaheuristics for air and space platforms.

Ismail Mohamed Hafez received the B.Sc. degree in electronics and electrical communications engineering from Ain Shams University, Cairo, Egypt, in 1983.

He was a Teaching Assistant in 1987, a Teacher in 1990, and an Assistant Professor in 1995 with Ain Shams University, where he has been a Professor since 2003. He is the Former Vice Dean of Community Service and Environmental Affairs and the Former Chairman of Electrical and Communication Engineering Department, Ain Shams University. His research interests include nanoelectronic devices, electronic circuits, and systems.

Fatma Newagy received the B.Sc., M.Sc. and Ph.D. in electronics and communications engineering from the Faculty of Engineering, Cairo University, Giza, Egypt, in 1998, 2002 and 2008, respectively.

She was a Research Assistant. She was an Assistant Professor with Cairo University from 2008 to 2011. Then, she moved to Ain Shams University as an Assistant Professor from 2011 to 2016, an Associate Professor from 2017 to 2022, and a Professor since 2022. She has been a member of the Space Research and Remote Sensing Scientific Council, Specialized Scientific Councils–Academy of Scientific Research and Technology since June 2018. She has been a Steering Committee Member of MIT – ASU Center of Excellence – Energy founded by USAID since April 2019. She shared different research projects and grants. Her research interests include UAV, smart grid, information theory, satellite communications, Internet of Things, mobile and wireless communications, and cognitive radio networks.